International Journal on Electrical Engineering and Informatics - Volume 17, Number 2, June 2025

# Induced Currents and Voltages by a Lightning Rod Down Conductors Inside a Protected Structure

Karim Belhoul and Slimane Bouazabia

Electrical and Industrial Systems Laboratory, Faculty of Electrical Engineering, University of Sciences and Technology Houari Boumediene, Algiers, Algeria

*Abstract:* A lightning protection system (LPS), such as a lightning rod, is designed to protect buildings, infrastructure, and people by safely channeling lightning's electrical discharge into the ground in a controlled manner. However, the lightning current flowing through the down conductors can create a disruptive electromagnetic environment inside the protected structure. Thus, modeling becomes necessary for their characterization. In this paper, an approach based on the transmission lines theory (TL) and the finite-difference time-domain method (FDTD) has been proposed to quantify electromagnetic transients inside the protected structure. The radiated electromagnetic field by the lightning's current flowing through the down conductors is used as forcing functions in Agrawal electromagnetic coupling equations. The induced currents and voltages on an overhead horizontal conductor inside the structure is calculated above a perfectly conducting ground. A Comparison with published results is conducted to assess the validity of the approach. Furthermore, the benefits of having one or two down conductors are explored and analyzed.

*Keywords:* Lightning, electromagnetic field, down conductors, induced current and voltage

## 1. Introduction

Due to lightning's destructive potential for infrastructure and electrical installations, lightning protection systems (LPS) play a critical role in risk reduction. The most common means of lightning protection remains the lightning rod.

The lightning rod is one of the most widely used lightning protection systems in the world. Due to its point effect, it attracts lightning and thus prevents its surroundings from being directly struck by the lightning leader. However, the presence of a lightning protection system can be dangerous for the environment to be protected. In fact, the forwarding of the lightning transient current through the down conductors to the grounding systems is often the source of electromagnetic compatibility (EMC) problems which should be taken into consideration.

Indeed, the current distribution along the down conductors emits an electromagnetic field liable to disturb the equipment inside the structure to be protected through induced currents and voltages [1 - 3].

Numerous studies have investigated through both computational modeling and experimental measurements the electromagnetic environment within structures during lightning strikes [4 – 9]. In recent research, the primary computational methods for analyzing the indoor electromagnetic environment during lightning strikes include the circuit-based approach, Method of Moments (MoM), and Finite-Difference Time-Domain (FDTD) technique. In the electric circuit-based approach, the system is partitioned into lumped-parameter circuits based on quasi-static approximations. However, this method requires intricate setup procedures and is computationally intensive. Additionally, it fails to account for the high-frequency components of lightning currents, limiting its accuracy [10 – 14]. While widely adopted, the Method of Moment involves computationally expensive matrix operations. Furthermore, time-domain results necessitate inverse Fourier transforms, and its frequency-domain solution of Maxwell's equations makes it unsuitable for wideband simulations due to inherent point-frequency limitations [1], [15]. The Finite-Difference Time-Domain (FDTD) method has also been employed to solve Maxwell's equations numerically [16], [17]. However, its application has been

Received: April 5th, 2025. Accepted: May 28th, 2025
DOI: 10.15676/ijeei.2025.17.2.3

largely restricted to simplified geometries due to the requirement for volumetric meshing of the entire computational domain, which results in prohibitively high computational costs.

These different authors present valuable observations and conclusion regarding the symmetrical arrangement of several down conductors, it minimizes the voltage drop induced in the protection system, reduces the voltage difference between the equipment connected to the down conductors system at different heights as well as the voltages that can electrocute people, and minimizes the magnetic field inside the structure to be protected [18 – 20] (the time variation of this magnetic field being potentially responsible for damaging the electronic equipment).

The passage of these transient currents in the down conductors is not without effect, the ground loop is often of large surface, the electromagnetic radiation of this one is generally found coupled to the various neighboring equipment and can cause stray currents by induction. It is therefore crucial to quantify and characterize this electromagnetic radiation in order to have at least optimal protection of the lightning protection system.

For filiform structures subjected to electromagnetic disturbances with frequency spectra below approximately 10 MHz (typical of lightning phenomena), the transmission lines approach is well suited for the study of electromagnetic coupling. In addition to the very acceptable accuracy of the results, it offers the advantage of easy implementation and acceptable calculation times. The coupling equations are solved using the finite-difference time-domain method (FDTD).

This case study examines a 50m-high x 10m-wide structure protected by a lightning rod installed at the geometric center of the roof, with singular down conductor grounding (figure1). A 10-meter-long power line, installed 1 meter above ground and spaced 10 meters horizontally from the down conductor, is subject to electromagnetic coupling from the transient fields generated by lightning current propagation along the down conductor. Terminations matching the line's characteristic impedance are applied to model realistic wave propagation.

The down conductors are modeled as vertical antennas above a perfectly conducting ground. Lightning current injection at down conductors' bases follows the Heidler function waveform formulation [21]. Current attenuation along down conductors is accounted for using MTL model [22] with an attenuation rate of $2\times10^3$ km.

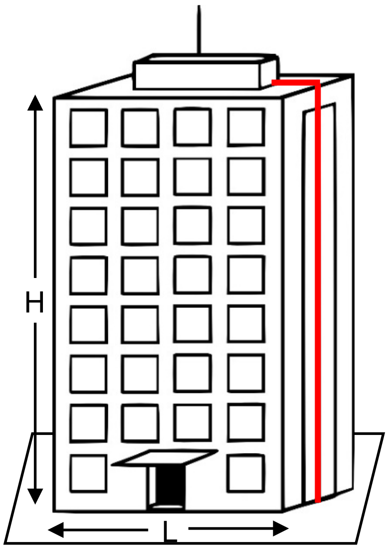


Figure 1. Studied structure with one down conductor (H=50m, L=10m)

## 2. Methodology

*A. Transmission Line Equations*

Transmission line theory provides the framework for analyzing electromagnetic wave propagation along linear conductive structures. The approach derives from a pair of coupled partial differential equations (telegrapher's equations) that govern the spatial and temporal evolution of voltage and current distributions along the conductor subject to the electromagnetic disturbance [23 – 26].

The coupling equations can be expressed in the form of three equivalent models [26 – 28]. For the case of a lossless line, the Agrawal coupling model [27] can be written in time domain as:

$$\frac{du^s(x,t)}{dx} + R.i(x,t) + L\frac{\partial i(x,t)}{\partial t} = E_x^e(x,h,t) \quad (1)$$

$$\frac{di(x,t)}{dx} + G.u^s(x,t) + C\frac{\partial u^s(x,t)}{\partial t} = 0 \quad (2)$$

Where:

$E_x^e(x,h,t)$ is the tangential component of the exciting electric field on the line;

*R, L, G, C* are respectively the resistance, inductance, conductance and linear capacitance of the line;

$u^s(x,t)$ is the diffracted voltage;

$i(x,t)$ is the induced current.

The boundary conditions expressed in terms of the diffracted voltage are given by:

$$u^s(0,t) = -Z_A.i(0,t) + \int_0^h E_z^e(0,z,t)dz \quad (3)$$

$$u^s(l,t) = Z_B.i(l,t) + \int_0^h E_z^e(l,z,t)dz \quad (4)$$

Where $Z_A$ and $Z_B$ are the termination impedances of the line.

The electric field components $E_x^e$ and $E_z^e$, radiated by the lightning current of the down conductor, were computed using the Hertzian dipole method. This analytical approach is derived by solving Maxwell's equations in terms of retarded scalar and vector potentials [29], [30]. The method is applicable in both the time and frequency domains. However, a direct time-domain solution is more suitable in our case, as it facilitates efficient handling [31]. The results of these electromagnetic field calculations were presented in [20].

*B. FDTD-Based Time-Domain Analysis of Coupling Equations*

The FDTD meshes are illustrated in figure 2. The conductor is subdivided alternately into current and voltage nodes; two consecutive nodes of the same type are separated by an interval Δx, and the two ends of the line are defined as voltage nodes.

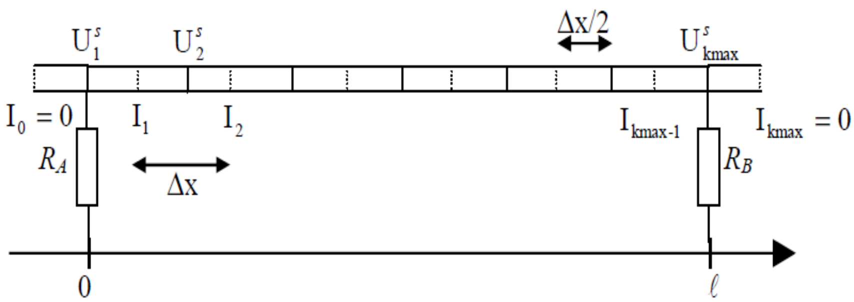


Figure 2. FDTD meshes on the line

The time and spatial meshes will be:

$$\begin{cases} (u^s)_k^n = v^s\big((k-1)\Delta x, n\Delta t\big) \\ (i)_k^n = i\big((k-1)\Delta x, n\Delta t\big) \\ (E_x^e)_k^n = E_x^e\big((k-1)\Delta x, n\Delta t, z=h\big) \end{cases} \quad (5)$$

with: $L = (k_{max} - 1)\Delta x$ and $t_{max} = n_{max}\Delta t$.

Using the Finite-Difference Time-Domain (FDTD) method and neglecting the convolution integral, we can discretize equations (1), (2), (3) and (4) and solve them directly in the time domain:

$$\frac{(u^s)_{k+1}^n - (u^s)_k^n}{\Delta x} + R\frac{(i)_{k+1/2}^{n+1/2} - (i)_{k+1/2}^{n-1/2}}{2} + L\frac{(i)_{k+1/2}^{n+1/2} - (i)_{k+1/2}^{n-1/2}}{\Delta t} = (E_x^e)_{k+1/2}^{n+1} \quad (6)$$

$$\frac{(i)_{k+1/2}^{n+1/2} - (i)_{k-1/2}^{n+1/2}}{\Delta x} + G\frac{(u^s)_k^{n+1} - (u^s)_k^n}{2} + C\frac{(u^s)_k^{n+1} - (u^s)_k^n}{\Delta t} = 0 \quad (7)$$

The solution is given by:

For k=1,…….,$k_{max}$-1 ;

$$(i)_{k+1/2}^{n+1/2} = \left[\frac{L}{\Delta t} + \frac{R}{2}\right]^{-1}\left\{(E_x^e)_{k+1/2}^{n+1} - \frac{(u^s)_{k+1}^n - (u^s)_k^n}{\Delta x} + \left[\frac{L}{\Delta t} + \frac{R}{2}\right](i)_{k+1/2}^{n-1/2}\right\} \quad (8)$$

For k=2,…….,$k_{max}$-1 ;

$$(u^s)_k^{n+1} = \left[\frac{C}{\Delta t} + \frac{G}{2}\right]^{-1}\frac{(i)_{k-1/2}^{n+1/2} - (i)_{k+1/2}^{n+1/2}}{\Delta x} + \left[\frac{C}{\Delta t} + \frac{G}{2}\right](u^s)_k^n \quad (9)$$

For the case of resistive terminations ($R_A$ et $R_B$), the boundaries conditions are :

$$(u^s)_1^{n+1} = \left[\frac{C}{\Delta t} + \frac{2\Delta x}{R_A}\right]^{-1}\left\{\frac{-(i)_{1/2}^{n+1/2}}{\Delta x} + \left[\frac{C}{\Delta t} + \frac{2\Delta x}{R_A}\right](u^s)_1^n\right\} \quad (10)$$

$$(u^s)_1^{n+1} = \left[\frac{C}{\Delta t} + \frac{2\Delta x}{R_A}\right]^{-1}\left\{\frac{-(i)_{1/2}^{n+1/2}}{\Delta x} + \left[\frac{C}{\Delta t} + \frac{2\Delta x}{R_A}\right](u^s)_1^n\right\} \quad (11)$$

For the stability of the FDTD, the time step Δt be smaller than the propagation time between two adjacent nodes as below:

$$\Delta t \le \frac{\Delta x}{v_p} \quad (12)$$

## 3. Results And Discussion

*A. Validation*

To verify the established model of the electromagnetic coupling, we consider the same configuration as reported by Rachidi [32]. He examined a system consisting of an overhead conductor 1 km in length, situated at a height of 10 meters above a perfectly conducting ground. The line is assumed to be terminated at its characteristic impedance at both ends. The radiating antenna (the lightning channel in this case) is considered symmetric relative to the two terminations and located at a distance of 50 meters from the line (Figure 3).

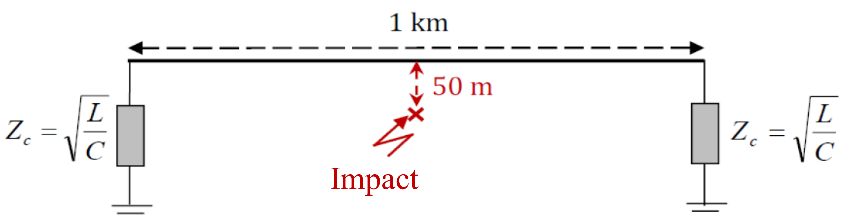


Figure 3. Geometry used by Rachidi [26]

The current at the base of the antenna has a peak value of 12 kA and is represented by the Heidler analytical function (table 1) [21]:

$$I(0,t) = \frac{I_0}{\eta} \frac{(t/\tau_1)^n}{1+(t/\tau_1)^n} \exp\left(\frac{-t}{\tau_2}\right) \qquad (13)$$

Its parameters values are given in the table below:

Table 1. Parameters of Heidler expression

| $I_{01}$(kA) | $\tau_{11}$(μs) | $\tau_{21}$(μs) | $n_1$ | $I_{02}$(kA) | $\tau_{12}$(μs) | $\tau_{22}$(μs) | $n_2$ |
|---|---|---|---|---|---|---|---|
| 10.7 | 0.25 | 2.5 | 2 | 6.5 | 2.1 | 230 | 2 |

The electromagnetic field is calculated using the dipole method starting from the current at the base of the channel defined above, using the MTL [22] model with an atypical value of λ = 1.7 km and a return stroke speed of v = 1.3 × $10^8$ m/s.

Here we compare our simulation results and those obtained by Rachidi.

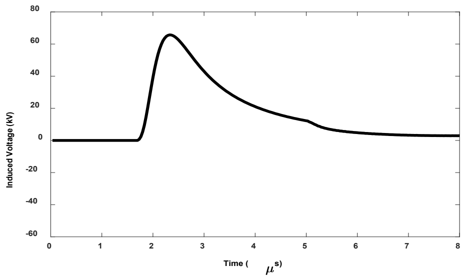


(a).

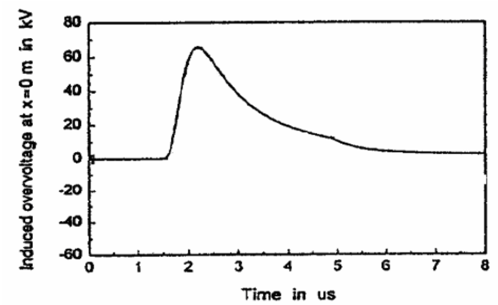


(b).

Figure 4. Induced voltage at the end of the overhead conductor
(a) Calculated (b) Published [32]

The computational results obtained from the model we adopted agrees with those reported by Rachidi [33]. Our results keep the general shape and amplitude compared to the published ones. These results validate the effectiveness of the transmission line formalism in assessing induced currents and voltages on overhead conductors caused by lightning-generated electromagnetic disturbances.

*B. Calculation of the Induced Currents and Voltages*

The considered structure is the same as the one described in figure 1. The electromagnetic field radiated by the down conductors carrying the lightning current will induce voltages and currents on the conductors located inside the structure. Moreover, the analysis focuses exclusively on the vertical part of the down conductors.

The conductor inside the structure affected by the electromagnetic field disturbance is a power line of 10m, positioned at a height of 1m above a perfectly conducting ground. The down conductor is located 10m from the end of the power line, which is terminated at its characteristic impedance at both ends. The latter ones results in the configuration illustrated in figure 5.

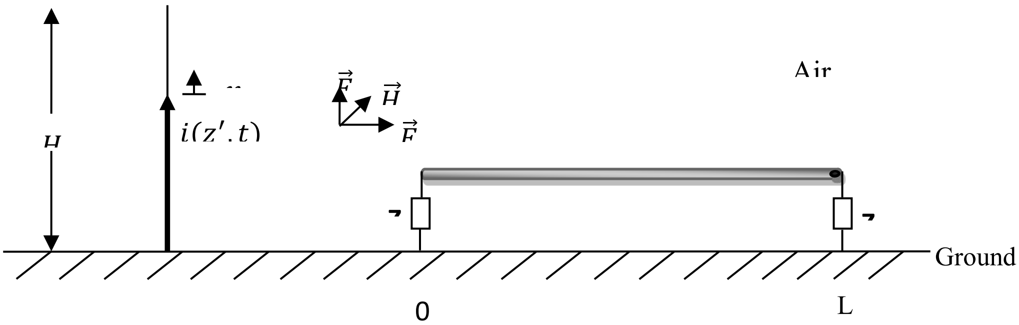


Figure 5. Single down conductor geometry for the calculation of induced voltages and currents

The induced current and voltage are illustrated in figure 6 and figure 7.

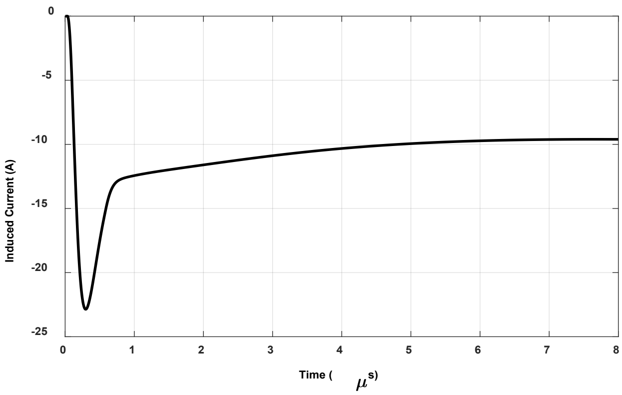


Figure 6. Induced current at the end of the line

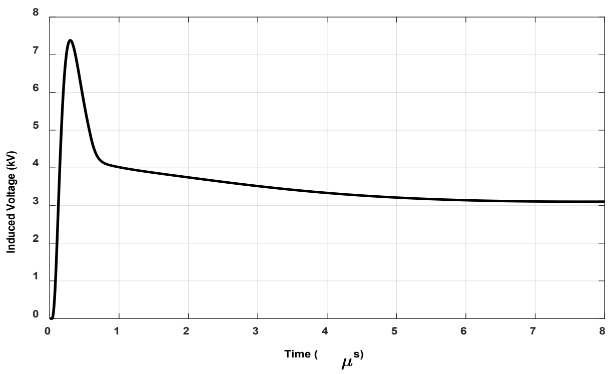


Figure 7. Induced voltage at the end of the line

The induced current and voltage at the end of the line in the presence of a single down conductor are significantly elevated. The calculated values (tens of kV and ~20A at line termination) indicate strong electromagnetic coupling between the down conductor and transmission line during lightning event.

To further investigate our findings within this configuration, we consider a power line with a length of 7m, placed at a height of 0.7m above a perfectly conducting ground. The down conductor is located at 3m from the end of the line.

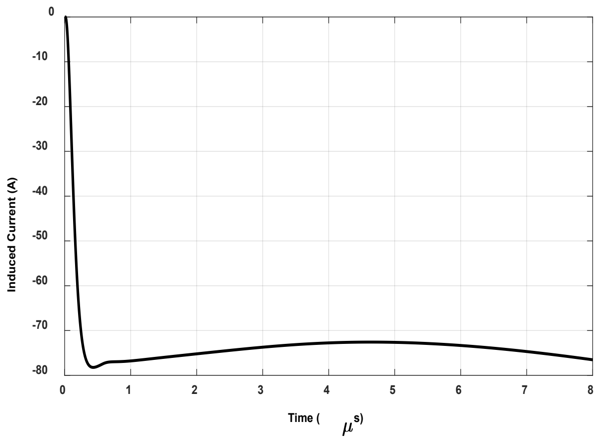


Figure 8. Induced current at the end of the line

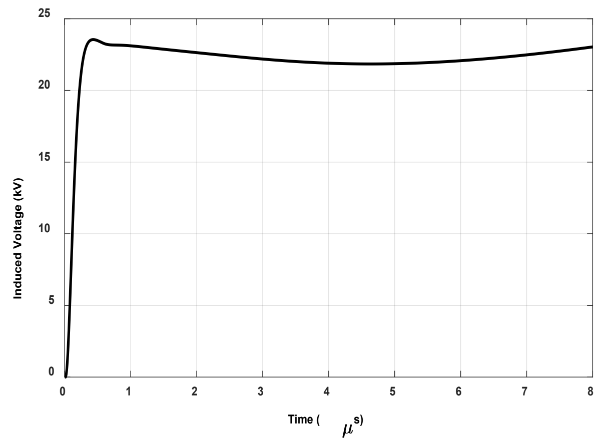


Figure 9. Induced voltage at the end of the line

The induced current and voltage are significantly higher than in the previous configuration as shown in table 2.

Table 2. Induced currents and voltages for both configuration

| Parameter | Config. A | Config. B | Increase |
|---|---|---|---|
| V_induced | 7.5 kV | 24 kV | 247.8% |
| I_induced | 23 A | 80 A | 220% |

The observed amplification of induced currents/voltages at the line termination exhibits two competing spatial dependencies: proximity enhancement effect (as the line approaches the down conductor, the induced effects gets higher) and line length attenuation paradox (shorter line show reduced induced effects).

In order to investigate the presence of a second down conductor's effect on the induced currents and voltages, we consider the same geometry described previously (figure 5), with a power line of 8m, at a height of 0.8m above a perfectly conducting ground and located 0.5m from the first down conductor, which means that the power line is located 1.5m from the second down conductor as shown in figure 10.

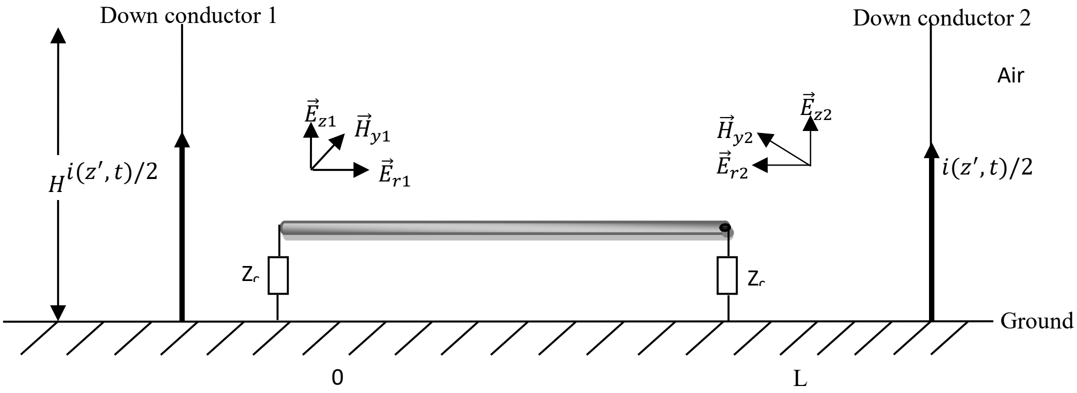


Figure 10. Two down conductors' geometry for the calculation of induced voltages and currents

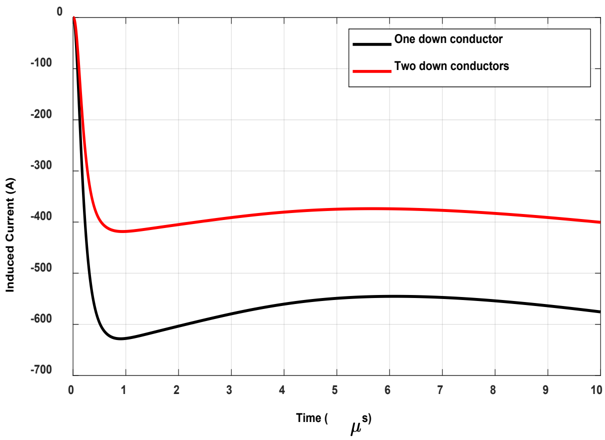


Figure 11. Induced current at the end of the line

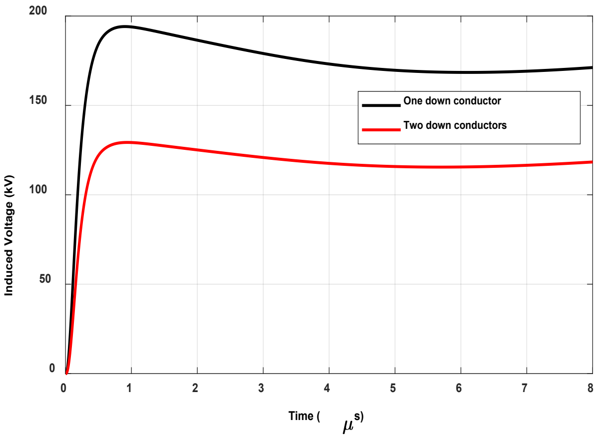


Figure 12. Induced voltage at the end of the line

The induced currents and voltages result from the combined electromagnetic field radiated by both down conductors as follows:

$$\begin{cases} \vec{E}_{rtot} = (E_{r1} - E_{r2})\,\overrightarrow{u_r} \\ \vec{E}_{ztot} = (E_{z1} + E_{z2})\,\overrightarrow{u_z} \\ \vec{H}_{\varphi tot} = \left(H_{\varphi 1} - H_{\varphi 2}\right)\overrightarrow{u_\varphi} \end{cases} \quad (14)$$

Figures 11 and 12 demonstrate that the introduction of a second down conductor significantly attenuates induced currents and voltages on the internal power line (between the two down conductors). However, despite this reduction, the residual induced values (130 kV and 400 A) remain critically high for electrical/electronic equipment, as they exceed standard withstand thresholds.

The following results present the peak induced voltages and currents along the power line within the structure (Fig. 10). To systematically evaluate the influence of down conductors, we analyze two configurations: (1) the baseline geometry and (2) a symmetric arrangement where the power line is positioned 1 m equidistant from both down conductors (ensuring identical coupling distances). Figures 13 and 14 illustrate the obtained results.

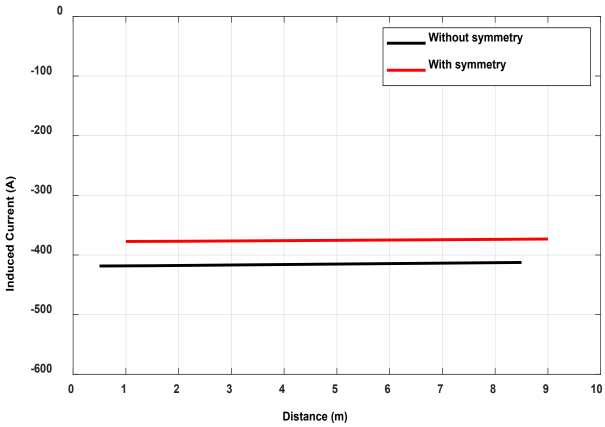


Figure 13. Induced current's peak values along the line

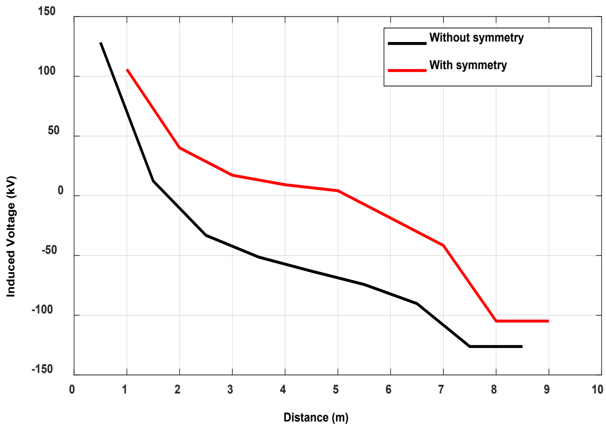


Figure 14. Induced voltage's peak values along the line

Figures 13 and 14 demonstrate that positioning the power line equidistant between both down conductors optimizes electromagnetic symmetry and significantly reduces induced transients compared to asymmetric configurations.

## 4. Conclusion

In this study, we proposed an approach to simulate the transient behavior of the down conductors of a lightning rod during a lightning event. This approach further enables the analysis of lightning-current's induced currents and voltages on an overhead conductor inside the protected structure. The proposed time-domain modeling approach uses the transmission line theory and the FDTD method. The latter allows easy modeling for thin-wire structure such as down conductors and overhead lines, and accurate interpretation of the results while simultaneously reducing the computational time. From the analysis carried out in this paper, it can be seen that the induced currents and voltages inside the structure are excessively high and strongly dependent on the geometric and physical parameters. Indeed, both the line-to-down conductor spatial configuration and the line's geometric characteristics are key determinants of induced electromagnetic effects. Somehow, the addition of a second down conductor significantly reduced the induced effects. Key observations include field cancellation effect, peak attenuation and practical implications, even though it remains too high for electrical equipment.

## 5. References


[1]. Orlandi, C. Mazzetti, Z. Flisowski, and M. Yarmarkin, "Systematic approach for the analysis of the electromagnetic environment inside a building during lightning strike", *IEEE Transactions on Electromagnetic Compatibility*, 40(4), 1998, 521–535.

[2]. I.A. Metwally and F.H. Heidler, "Improvement of the lightning shielding performance of overhead transmission lines by passive shield wires", *IEEE Transactions on Electromagnetic Compatibility*, 45(2), 2003, 378–392.

[3]. M. A. Uman, "The art and science of lightning protection", Cambridge University Press, New York, 2008.

[4]. A. Sowa, Surge current distribution in building during a direct lightning stroke, Proc. *IEEE Int. Symp. Electromagn. Compat, USA*, 1991, 248–252.

[5]. F.K. Chew, M.R.M. Esa, and H. Ahmad, Dispersion of standard and nonstandard lightning current to ground in a telecommunication building, *Int. Power Eng. Conf., Singapore*, 2007, 207–212.

[6]. J. Kato, H. Kawano, T. Tominaga, and S. Kuramoto, Investigation of lightning surge current induced in reinforced concrete buildings by direct strikes, *Int. Symp. Lightning Prot. EMC*, Tokyo, Japan, 2001.

[7]. F. Lei and Z. Peibai, The digital model of high building struck by lightning, *High Voltage Apparatus*, 36(6), 2000, 3–7.

[8]. F. Lei and Z. Peibai, Computation of the induced electric field in a high building, *High Voltage Engineering*, 27(1), 2001, 52–54.

[9]. Z. Xiaoqing, C. Shuiming, and W. Weihan, Lightning transient responses involving frequency-dependent characteristics in the building steel structure, *Journal of Tsinghua University (Science Technology)*, 37(6), 1997, 103–107.

[10]. C.A.F. Sartori and A. Orlandi, Optimization of the LPS configuration for minimization of the radiated electromagnetic field, Proc. *IEEE Int. Symp. Electromagn. Compat, Washington, USA*, 2, 2000, 827–832.

[11]. C.A.F. Sartori, J.R. Cardoso, et al., Constrained decision planning applied to field profile optimization in LPS of structures directly struck by lightning, *IEEE Transactions on Magnetics*, 38, 2002, 757–760.

[12]. W. Qing, F. Zhengcai, et al., Influence of tightening current waveform on magnetic fields in a building struck by lightning, *High Voltage Engineering*, 27, 2001, 7–9.

[13]. H. Wei, H. Jianming, et al., The electromagnetic field in the building struck by lightning, *Ship Electronic Engineering*, 24, 2004, 270–272.

[14]. J. Yafei, Z. Ke, et al., Calculation of the maximum magnetic field inside the lightning protection system of a building, *High Voltage Engineering*, 35, 2009, 914–918.

[15]. I.A. Metwally, W.J. Zischank, and F.H. Heidler, Measurement of magnetic fields inside single- and double-layer reinforced concrete buildings during simulated lightning currents, *IEEE Transactions on Electromagnetic Compatibility*, 46, 2004, 208–221.

[16]. Y. Baba and V.A. Rakov, Voltages induced on an overhead wire by lightning strikes to a nearby tall grounded object, *IEEE Transactions on Electromagnetic Compatibility*, 48(1), 212–224, 2006.

[17]. H.M. Ren, B.H. Zhou, V.A. Rakov, L.H. Shi, C. Gao, and J.H. Yang, Analysis of lightning-induced voltages on overhead lines using a 2-D FDTD method and Agrawal coupling model, *IEEE Transactions on Electromagnetic Compatibility*, 50(3), 2008, 651–569.

[18]. Berger, K. and Vogelsanger, "Photographische blitzuntersuchungen der jahre 1955–196 auf dem monte San Salvatore", Bull. Schweiz Elektrotech. Ver. 57: 599–620, E. 1966.

[19]. Berger, K. and Vogelsanger, "New results of lightning observations", In Planetary Electrodynamics, ed. S. C. Coroniti and J. Hughes. New York: Gordon and Breach, pp. 489 510, E. 1969.

[20]. K. Belhoul and S. Bouazabia. (2013). Analysis Of The Electromagnetic Environment Engendered Inside A Building By A Lightning Protection System (LPS). *International Journal of Power and Energy Systems*, 33(4).

[21]. F. Heidler, Analytische Blitzstorm-Funktion zur LEMPBerechnung, Paper 1.9, Munich, Septembre 16–20, 1985, 63–66.

[22]. C.A. Nucci, C. Mazzetti, F. Rachidi, and M. Ianoz, On lightning return stroke models for LEMP calculations, *Proc. 19th International Conference on Lightning Protection*, 1988, Graz.

[23]. F. Rachidi, "Analyse de couplage avec les lignes de transmission", Compatibilité électromagnétique, Note de cours, EPFL de Lausanne, Suisse, été 2006.

[24]. F. Rachidi and S. V. Tkachenko, "Advances in electrical engineering and electromagnetics", WIT Press, 2008.

[25]. C. R. Paul, "Analysis of multiconductor transmission lines", Wiley Interscience, 1994.

[26]. C. D. Taylor, R. S. Satterwhite, W. Jr. Harrison, "The response of terminated two-wire transmission line excited by a nonuniform electromagnetic field", *IEEE Trans. On Antennas and propagation*, vol. AP-13, pp.987-989, 1965.

[27]. A. K. Agrawal, H.J. Price, S.H. Gurbaxani, "Transient Response of multiconductor transmission lines excited by a nonuniform electromagnetic field", *IEEE Trans. On Electromagnetic Compatibility. EMC-22*, pp. 119-129, 1980.

[28]. F. Rachidi, "Formulation of the field to transmission line coupling equations in terms of magnetic excitation field", *IEEE Trans. On Electromagnetic Compatibility, Vol. EMC-*35, N°. 3, pp. 404-407, 1993.

[29]. M.J. Master and M.A. Uman, Transient electric and magnetic fields associated with establishing a finite electrostatic dipole, *American Journal of Physics*, 51, 1983, 118–126.

[30]. M. Rubinstein and M.A. Uman, Methods for calculating the electromagnetic fields from a known source distribution: Application to lightning, *IEEE Transactions on Electromagnetic Compatibility*, 31(2), 1989, 183–189.

[31]. M. Paolone, et al., Lightning electromagnetic field coupling to overhead lines: theory, numerical simulations, and experimental validation, *IEEE Transactions on Electromagnetic Compatibility*, 51(3), 2009, 532–547.

[32]. F. Rachidi, "Effets électromagnétiques de la foudre sur les lignes de transmission aériennes : Modélisation et Simulation", *Thèse de Doctorat, Ecole polytechnique Fédérale de Lausanne*, 1991.

**Karim Belhoul** received his Ph.D degree in Electrical Engineering from University of Sciences and Technology Houari Boumediene. Since 2019, he has been with the Faculty of Electrical Engineering, USTHB, Algiers. His research interests include lightning physics and electromagnetic compatibility.

**Slimane Bouazabia** received his Phd Doctorate in Polytechnic School of Algiers. His interest domains are high voltage technology, electrical discharges, electricomagnetic field calculation. Since 1988, he has assumed the role of professor (teaching and research) at Algiers University USTHB.